Original Article

Identification of phosphodiesterase-4 as the therapeutic target of arctigenin in alleviating psoriatic skin inflammation

Heng Li [a,b,1], Xianglei Zhang [b,c,1], Caigui Xiang [a,b], Chunlan Feng [a], Chen Fan [a], Moting Liu [a,b], Huimin Lu [a,b], Haixia Su [b,c], Yu Zhou [a], Qing Qi [a], Yechun Xu [b,c,*], Wei Tang [a,b,*]

[a] Laboratory of Anti-inflammation and Immunopharmacology, Shanghai Institute of Materia Medica, Chinese Academy of Sciences, Shanghai 201203, China
[b] School of Pharmacy, University of Chinese Academy of Sciences, Beijing 100049, China
[c] CAS Key Laboratory of Receptor Research, Drug Discovery and Design Center, Shanghai Institute of Materia Medica, Chinese Academy of Sciences, Shanghai 201203, China

ABSTRACT

Introduction: Arctigenin, derived from Arctium lappa L., has multiple pharmacological activities, including immunoregulatory, anti-diabetic, anti-tumor, and neuroprotective effects. Nevertheless, the potential therapeutic target of arctigenin in modulating inflammation remains undefined.
Objectives: In the present study, we identified that arctigenin was a phosphodiesterase-4 (PDE4) selective inhibitor for the first time. Further investigations were performed to fully uncover the effects and mechanism of arctigenin on experimental murine psoriasis model.
Methods: Crystal structure determination, PDEs enzyme assay, and isothermal titration calorimetry were included to illustrate the binding specialty, inhibitory effects, and selectivity of arctigenin on PDE4D. The anti-inflammatory effects were conducted in LPS-activated human peripheral blood mononuclear cells (PBMCs) and RAW264.7 cells. Imiquimod-induced murine psoriasis was performed to uncover the therapeutic effects and mechanism of arctigenin in vivo.
Results: Arctigenin could bind to the catalytic domain of PDE4D via formation of hydrogen bonds as well as - stacking interactions between the dibenzyl butyrolactone of arctigenin and several residues of PDE4D. Accordingly, arctigenin showed prominent anti-inflammation in human PBMCs and murine RAW264.7 cells. PDE4 inhibition by arctigenin resulted in elevation of intracellular cyclic adenosine monophosphate (cAMP) and phosphorylation of cAMP-response element binding protein (CREB), which were largely blocked through intervention of protein kinase A (PKA) activity by H89 treatment or reduction of protein expression by siRNA transfection. Moreover, we first identified that a topical application of arctigenin ameliorated experimental psoriatic manifestations in imiquimod-induced murine psoriasis model by decreasing adhesion and chemotaxis of several inflammatory cells. Further proteomics analysis revealed that arctigenin could rectify the immune dysfunction and hyperactivation of keratinocytes in the inflamed skin microenvironments, which might be largely related to the expression of Keratins.
Conclusion: The research provided credible clew that inhibition of PDE4 by arctigenin might function as the potential therapeutic approach for the treatment of psoriasis.

Introduction

Traditional Chinese medicine (TCM) offers a vast treasury of pharmaceutical candidates in modulating immune homeostasis and treating inflammatory diseases [1–3]. Arctigenin, a phenyl-propanoid dibenzyl butyrolactone lignan, is one major active ingredient extracted from the fruits and seeds of Arctium lappa L., which has been rifely applied in clinical for anti-influenza and metabolic diseases in Asia [4]. Accumulating evidences have extensively revealed that arctigenin possessed therapeutic efficacies in numerous diseases, such as acute lung and liver injury [5–7], autoimmune hepatitis [8], inflammatory bowel diseases [9–11], and multiple sclerosis [12], which were largely accompanied by suppressing the abnormal activation of immune cells and modulating conventional inflammatory signaling pathways. Nevertheless, the molecular mechanism and potential targets of arctigenin in regulating inflammation remain elusive.

Phosphodiesterases (PDEs) act as the intracellular enzymes, hydrolyzing the cyclic adenosine monophosphate (cAMP) and cyclic guanosine monophosphate (cGMP), which are second messengers and modulators of various physiological processes [13,14]. Significant upregulation of PDE4 activity and distribution was observed in the peripheral immune cells and impaired skin biopsies in patients with psoriasis and other inflammatory diseases [15,16]. Accumulating evidences have demonstrated that inhibition of PDE4 resulted in significant upregulation of cAMP and subsequent activation of protein kinase A (PKA) [17,18]. Thereafter, phosphorylation of nuclear transcriptional factors, such as cAMP-responsive element binding protein (CREB), cAMP responsive element modulator (CREM), and activated transcription factor 1 (ATF-1), collectively regulated inflammation and tissue homeostasis. In the past decades, PDE4-targeted drug discovery has been widely accepted as a competitive and promising strategy for anti-inflammatory agents' design. Roflumilast, apremilast, and crisaborole have been licensed for patients who suffered from chronic obstructive pulmonary disease (COPD), psoriatic arthritis (PsA), and atopic dermatitis, respectively [19].

Psoriasis, with a high incidence worldwide, is an autoimmune disease, which refers to something wrong with the body's immune system. It is a multifactorial and inflammatory skin disorder that is distinguished by the local formation of silver plaques and skin abnormal thickness [20]. The pathological mechanism of psoriasis is closely associated with the communication between primary tissue-resident and newly-recruited inflammatory cells, including macrophages, dendritic cells (DCs), and activated T cells, along with the increased production of corresponding cytokines and chemokines [21,22]. Upon exposure to the internal and external harmful stimulus, including physical trauma, bacterial infection, and endotoxins, inflammatory cells are activated to overexpress interferon-γ (IFN-γ), tumor necrosis factor-α (TNF-α), interleukin-12 (IL-12), IL-17A and IL-23, leading to excessive proliferation of keratinocytes [23,24]. In addition, the abnormal expression of chemokines and adhesion molecules derived from keratinocytes, in turn, will promote the infiltration of an additional variety of immune cells, thereby exacerbating the inflammatory environment of the skin psoriasis.

In the present study, co-crystallization and isothermal titration calorimetry were performed to uncover the binding properties of arctigenin with the catalytic domain of PDE4D. Further functional verifications were performed, including PDEs enzymic inhibition assay, and inflammatory mediator production from human peripheral blood mononuclear cells (PBMCs) and RAW264.7 cells. Moreover, an imiquimod (IMQ)-induced experimental psoriasis model was conducted to explore the efficacies and potential mechanism of arctigenin.

Materials and methods

Crystal structure determination

The protein co-crystallization of the PDE4D catalytic domain in complex with arctigenin was performed by the protocols reported previously [25]. The X-ray diffraction data were collected and analyzed at the Shanghai Synchrotron Radiation Facility (SSRF, BL17U1, PILATUS 6 M detector). The relevant data of refinement statistics are given in Supplementary Table S1.

PDEs enzyme assay

The enzymatic activity of the purified catalytic domain of PDE4D, PDE5A, PDE7A, PDE9A, and PDE10A, and full-length PDE1A, PDE2A, PDE3A, PDE6C, PDE8A, and PDE11A, purchased from BPS Bioscience (San Diego, CA, USA), was performed by determining the biochemical hydrolysis of [3H]-cAMP or [3H]-cGMP into [3H]-AMP or [3H]-GMP, respectively, using the scintillation proximity assay (SPA) as described previously [25]. The enzymatic activities in RAW264.7 cells and skin biopsies were normalized to the concentration of total proteins.

Isothermal titration calorimetry

The binding thermodynamic profile of arctigenin to PDE4D catalytic domain was measured by the isothermal titration calorimetry (ITC) method using the iTC-200 calorimeter (Little Chalfont, Buckinghamshire, UK) as described previously [25]. The enthalpy change and association constant were obtained by nonlinear regression of the data using Origin software (San Clemente, CA, USA).

PDK1 kinase assay

For measurement of the inhibitory effect of arctigenin on PDK1, we used a PDK1 kinase enzyme assay (V2761, Promega (Beijing) Biotech, China) from Promega according to the manufacturer's instruction. Recombinant full-length human PDK1, ATP, substrate and tested compounds were diluted with kinase buffer that comprised 40 mM Tris (pH 7.5), 20 mM $MgCl_2$, 0.1 mg/mL BSA, and 50 μM DTT to a concentration of 20 nM, 1 ng/μL, 20 μM and from 100 μM to 10 nM, respectively, before adding to the wells of 384 low volume plate. After incubating at room temperature for 60 min, 5 μL of ADP-Glo™ reagent was added to each well of plate and incubated at room temperature for another 40 min. Then adding 10 μL of kinase detection reagent and incubating at room temperature for 30 min before recording luminescence with the Bio-Tek Synergy4 plate reader.

Lipopolysaccharide stimulation of human PBMCs

The inhibitory activity of arctigenin on lipopolysaccharide (LPS, Sigma-Aldrich, St. Louis, MO, USA) stimulated human PBMCs was assayed as previously reported [25]. Human PBMCs (1×10^6/well) were purchased from SAILY BIO (Shanghai, China) and maintained in the RPMI-1640 medium (Gibco, Grand Island, NY, USA) in the presence of 10% FBS (Gibco) and 2 mM L-glutamine.

Establishment and assessment of IMQ-induced murine psoriatic skin lesions

Female wild-type BALB/c mice (6–8 weeks old, 20–22 g) were acquired from Shanghai Laboratory Animal Center of the Chinese Academy of Sciences. Mice were fed with standard laboratory chow and water under the specific pathogen-free (SPF) facility with 12 h of light/12 h of dark cycle, 24 ± 2 °C and 55 ± 5% relative humidity. All experiments in the present study were conducted as the previous description according to the National Institutes of Health (NIH) Guide for Care and Use of Laboratory Animals in compliance with the ARRIVE guidelines and were approved by the Bioethics Committee of the Shanghai Institute of Materia Medica (SIMM), Chinese Academy of Sciences (CAS) [26].

The dorsal skins of female mice were shaved with an electric razor and depilatory creams. Then, all mice were randomly divided into 3 independent experimental groups (n = 7 mice per group), namely normal, vehicle (IMQ-treated only), and arctigenin treatment (IMQ with 5% arctigenin cream). The psoriatic inflammatory skin lesions were established by topical application with 62.5 mg daily of 0.05% IMQ cream (Sichuan Mingxin Pharmaceutical, Sichuan, China) on the shaved back skin for 7 successive days. In

the course of arctigenin treatment, murine body weight in each group and skin inflammatory scores, referring to Psoriasis Area and Severity Index (PASI, Supplementary Table S2), were monitored blind by 3 investigators, as previous description [27].

Histological examination

Skin sections were fixed in 4% formaldehyde buffered in PBS solution and then embedded in paraffin. Subsequently, 3 μm sections were cut and stained with hematoxylin and eosin (H&E) reagents. The representative pictures were observed and obtained under a light microscope (Olympus IX73, Tokyo, Japan). Accordingly, the epidermal thickness in all groups was calculated and recorded by the distance between the interfollicular epidermis by using the Image-Pro Plus software (Silver Springs, MD, USA).

Protein extraction, quantization, and LC-MS/MS analysis

The skin samples from three groups were transferred into low protein binding tubes and lysed with digestion buffer. Digested peptides were centrifuged at 12000 rpm for 20 min and collected for further Tandem Mass Tags (TMT)-labeling as following: Normal groups, TMT^{10}-126, TMT^{10}-127 N, TMT^{10}-127C; Vehicle groups, TMT^{10}-128 N, TMT^{10}-128C, TMT^{10}-129 N; Arctigenin groups, TMT^{10}-129C, TMT^{10}-130 N, TMT^{10}-130C; Group Mix, TMT^{10}-131.

All proteomic analyses were conducted by the Q-Exactive HF mass spectrometer (Thermo Fisher Scientific). Samples were then separated by a C18 column (15 cm × 75 μm) on an EASY-nLC^{TM} 1200 system (Thermo Fisher Scientific). ProteomeDiscoverer (v.2.3, Thermo Fisher Scientific) was used to search all the raw data thoroughly against the sample protein database (uniprot-reviewed-Mus musculus (Mouse)-201908.fasta). Functional analyses, including the Gene Ontology (GO) enrichment analysis and Kyoto Encyclopedia of Genes and Genomes (KEGG) pathway analysis were performed on the QuickGO and KEGG database, respectively.

Flow cytometry analysis

Skin single cell suspensions from the inflamed biopsies were prepared and isolated as the previous description [28,29]. In brief, skin samples were minced and digested with collagenase IV (1 mg/mL, Sigma-Aldrich) in the RMPI-1640 media supplemented with 10% FBS at 37 °C incubator for 2.5 h, and subsequently filtered through a 70-μm mesh to acquire the single cells. The skin cell suspensions were washed twice with cold PBS and then incubated with FVD eFluor^{TM} 780 (Thermo Fisher Scientific) at 4 °C for 30 min to differentiate the viable cells from dead cells. Upon being blocked by staining with anti-CD16/CD32 mAb (Thermo Fisher Scientific), cells were further incubated with fluorescein isothiocyanate (FITC), phycoerythrin (PE), peridinin-chlorophyll proteins-Cyanine5.5 (Percp-Cy5.5), allophycocyanin (APC), brilliant violet 421 (BV421), and brilliant ultraviolet 395 (BUV395)-conjugated antibodies. Data were analyzed using FlowJo software (Tree Star, Ashland, OR, USA).

Cell cultures and treatment

RAW264.7 cells, murine macrophage cell line, were obtained from the American Type Culture Collection (ATCC, Manassas, VA, USA) and maintained in Dulbecco's modified Eagle's media (DMEM, Gibco) containing 10% FBS (Hyclone), 2 mM of L-glutamine, 100 U/mL penicillin, and 100 μg/mL streptomycin in a humidified incubator of 5% CO_2 at 37 °C. To reveal the anti-inflammatory effects of arctigenin on RAW264.7 cells, cells were treated with arctigenin (100, 30, and 10 μM) upon LPS induction

(1 μg/mL, Sigma-Aldrich). After additional 15 min incubation, RAW264.7 cells were lysed for following western blotting assay and for RT-PCR assay after 3 h incubation. Meanwhile, the supernatants were centrifuged and stored for inflammatory cytokines, TNF-α, and NO measurement. To further confirm the critical role of PKA-CREB signaling in the effects of arctigenin, RAW264.7 cells were incubated with arctigenin (100 μM), H89 (10 μM, an inhibitor of PKA, Selleck Chemicals, Houston, TX, USA), and/or forskolin (10 μM, an activator of adenylyl cyclase, Sigma-Aldrich) for 15 min and then cells were collected for western blotting analysis. Subsequently, to decrease the protein expression of PKA in RAW264.7 cells, siRNA targeting for PKA C-α gene silence (Cell Signaling Technology) was mixed with Lipofectamine® RNAiMAX reagent (Thermo Fisher Scientific) in serum-free opti-MEM medium (Gibco) and added into the cells for 72 h transfection.

ELISA and Luminex assay

Serum inflammatory cytokines were quantified by the Luminex 200 instrument (Merck Millipore, Billerica, MA, USA) using a Th1/Th2/Th9/Th17/Th22/Treg Cytokine 17-Plex Mouse ProcartaPlex^{TM} Panel (Thermo Fisher Scientific). Cytokines in RAW264.7 cell supernatants were analyzed by mouse TNF-α and IL-6 ELISA kits (BD Biosciences, San Diego, CA, USA) as described previously [16]. For cAMP detection, cells and psoriatic skin biopsies were lysed and isolated by 0.1 M HCl and the intracellular cAMP level was quantified by using the direct cAMP ELISA kits (Enzo Life Sciences, The Netherlands) according to the directions.

Immunofluorescence and immunohistochemistry

For immunofluorescent evaluation, cells were fixed in 4% formaldehyde, blocked with the BSA blocking buffer (Beyotime Biotechnology, Shanghai, China), and stained at 4 °C overnight with phospho-CREB antibodies (Cell Signaling Technology). The skin slices were then incubated with FITC-conjugated goat anti-rabbit secondary antibodies and counterstained with DAPI to stain the nuclei of RAW264.7 cells. For immunochemistry analysis, paraffin-embedded skin tissue slices were blocked with 3% H_2O_2 solution, retrieved by citrate buffer solution and then incubated at 4 °C overnight with anti-Ki-67 antibodies (Abcam, Cambridge, UK), and CD3 Abs (Abcam). Then, the positive signals were visualized by biotinylated horse anti-rabbit secondary antibodies and streptavidin horseradish peroxidase. The representative pictures were obtained using the light microscope (Olympus IX73 microscope).

RNA extraction and RT-PCR

Total RNA from the murine skin biopsies and RAW264.7 cells was isolated and purified by using the RNAsimple total RNA kits (Tiangen). Subsequently, total RNA (500 ng per unit) was reversely transcribed by the Hifair^{TM} 1st Strand cDNA Synthesis SuperMix regents (Yeasen, Shanghai, China) with consecutive incubation of 25 °C for 5 min, 42 °C for 30 min. and 85 °C for 5 min. Real-time quantitative PCR analyses were conducted with the SYBR® Green Realtime PCR Master Mix regents (Yeasen) according to the directions on the 7500 Fast Real-Time PCR System (Applied Biosystems, Foster city, CA, USA) for PCR amplification with holding stage (95 °C for 30 s), cycling stage (95 °C for 15 s and 60 °C for 34 s for 40 cycles), and melt curve stage using the gene-specific primers in Supplementary Table S3 by the ΔΔ Ct method.

Western blotting assay

The protein concentrations from the inflamed skin biopsies and RAW264.7 cells were measured and quantified by the Pierce BCA protein assay kits (Thermo Fisher Scientific). The equal protein amounts were dissolved in the SDS-loading buffer and subjected to 10% electrophoretic SDS-PAGE, then transferred into the nitrocellulose membranes (Bio-Rad, Hercules, CA, USA). The nitrocellulose membranes were blocked for 10 min at room temperature with SuperBlock T20 blocking buffer (Thermo Fisher Scientific) and then incubated at 4 °C overnight with primary antibodies. The positive signals were visualized by using the SuperSignal West Femto Maximum Sensitivity Substrate (Thermo Fisher Scientific) under the exposure of ChemiDoc™ MP Imaging System (Bio-Rad).

Statistical analysis

All data in the present research were shown as mean ± SEM and the statistical variations were performed by using one-way ANOVA (3 and more groups) or Student's t-test (2 groups) with Dunnet's multiple comparisons test with no significant variance inhomogeneity by GraphPad Prism (GraphPad Software, Version 6.0, LLC, CA, USA). P-values of<0.05 ($p < 0.05$) were regarded as statistical significance.

Results

Arctigenin could specifically bind to the catalytic domain of PDE4D

To discover novel PDE4 inhibitors, we screened our in-house natural products library containing ~ 500 natural products with good solubility and drug-like properties by a scintillation proximity assay (SPA) and found that arctigenin showed an acceptable physicochemical property (Table S4) and moderate inhibitory activity toward PDE4D with an IC_{50} of 3.76 ± 0.28 μM (Fig. 1A). As illustrated in Fig. 1B, the dimethoxybenzene ring of arctigenin formed two hydrogen bonds with the conserved Q369, and a face-to-face $\pi - \pi$ interaction with F372. H160 at the metal binding site formed another hydrogen bond with arctigenin (Fig. 1B). The inhibitory activity as well as the binding mode of arctigenin were well consistent with the thermodynamic properties of arctigenin revealed by the ITC analysis, which suggested the enthalpy contribution is dominant for binding of arctigenin to the catalytic domain of PDE4D with a single digit micromolar binding affinity (Fig. 1C and Table S5).

Arctigenin was highly specific and selective for PDE4 inhibition

Previously, it has been indicated that arctigenin could modulate the PDK1/AKT/PDE4D axis in asthma therapy [30]. We intended to uncover the direct binding of arctigenin with PDK1, whereas the measured inhibition of arctigenin on PDK1 seemed negligible, compared with that of a known PDK1 inhibitor, GSK2334470 (Table S6). The selectivity of arctigenin against other PDE families was also measured. Arctigenin showed weak inhibitory activities against PDE1A, PDE2A, PDE3A, PDE5A, PDE6C, PDE7A, PDE8A, PDE9A, and PDE11A (Table S7). These data indicate that arctigenin is not a PDK1 inhibitor but a PDE4 inhibitor with a relatively high selectivity over other PDEs.

Arctigenin suppressed the secretion of inflammatory mediators in vitro

Since PDE4 was highly expressed in immune cells, arctigenin was further evaluated for the inhibitory activity on the TNF-α production from the LPS-stimulated human PBMCs. As shown in Fig. 1D, arctigenin suppressed the TNF-α production with an IC_{50} of 35.18 ± 6.01 μM. To further confirm the anti-inflammation effects of arctigenin, murine RAW264.7 cells were included in the current research. Arctigenin could dose-dependently (100, 30, and 10 μM) reduce the production of TNF-α and IL-6 from LPS-induced RAW264.7 cells, which was not associated with the cytotoxicity of arctigenin (Fig. S1). Conformably, arctigenin also decreased the mRNA expression level of TNF-α and IL-6 in RAW264.7 cells (Fig. S2A-B). Moreover, arctigenin downregulated the inflammatory mediators, iNOS and COX-2, in a concentration-dependent manner (Fig. S2C), which was in line with the previous report [31]. Consequently, the accumulation of nitrite, the stable and product of NO by RAW264.7 cells, was dramatically reduced following incubation with arctigenin (Fig. S2D).

Arctigenin activated cAMP-dependent phosphorylation of CREB in RAW264.7 cells

Due to the direct PDE4 inhibition by arctigenin, we further aimed to find out whether arctigenin displayed direct effects of PDE4-mediated signaling pathway in regulating inflammation [32]. Prospectively, arctigenin addition led to significant elevation of intracellular cAMP in RAW264.7 cells in a concentration-dependent manner (Fig. S2E). Linked with previous research, cAMP accumulation by arctigenin subsequently led to the phosphorylation of CREB without any effects on the total expression level of CREB and PKA protein (Fig. 2A and Fig. S3A). The results were confirmed by immunofluorescent staining with phospho-CREB, which showed that localization of phospho-CREB largely co-existed with the nuclei of RAW264.7 cells (Fig. 2B).

We further found that H89 intervention obviously blocked the effects of arctigenin on phosphorylation of CREB, whereas, the adenylyl cyclase activator, forskolin, could further enhance the effects of arctigenin on promoting the phosphorylation of CREB (Fig. 2C and Fig. S3B). Further biological investigation confirmed the function of arctigenin on the secretion of TNF-α (Fig. 2D). Accordingly, siRNA targeting for reducing the expression of PKA were transfected, compared with NC controls, the protein level of PKA was mostly decreased in transfected-RAW264.7 cells (Fig. 2E and Fig. S3C). In line with the effects of H89 treatment, phosphorylation of CREB and inhibition of TNF-α secretion were hindered whether the cells were incubated with arctigenin and/or forskolin (Fig. 2E and 2F). In brief, our research indicated PKA functioned as the crucial factor in the anti-inflammation of arctigenin.

Topical application of arctigenin significantly alleviated IMQ-induced psoriatic skin inflammation

Given the anti-inflammatory activity and intrinsic physico-chemical property of arctigenin, we therefore uncovered the potential therapeutic effects of arctigenin in IMQ-induced murine psoriatic skin lesions. As demonstrated in Fig. 3A-D, upon topical application of IMQ cream, severe body weight loss, typical skin lesions, including scales, thickness, and erythema appeared. Therapeutically, topical application of arctigenin treatment (5% specification) significantly reversed the body weight loss and attenuated the experimental manifestations and decreased the cumulative PASI scores of the shaved skin (Fig. 3A-D). Histologically, arctigenin treatment dramatically improved the epidermal thickening and immune cells recruitment in the inflamed tissue microenvironments (Fig. 3E-F). In addition, arctigenin could ameliorate the concomitant splenomegaly (Fig. 3G). Further immunohistochemistry with Ki-67 also elucidated hyperplasia of cuticular layers and the positive staining signals in the epidermis were reduced following arctigenin treatment (Fig. 3H). Moreover, Luminex assay of serum cytokines showed that arctigenin could reduce the production of
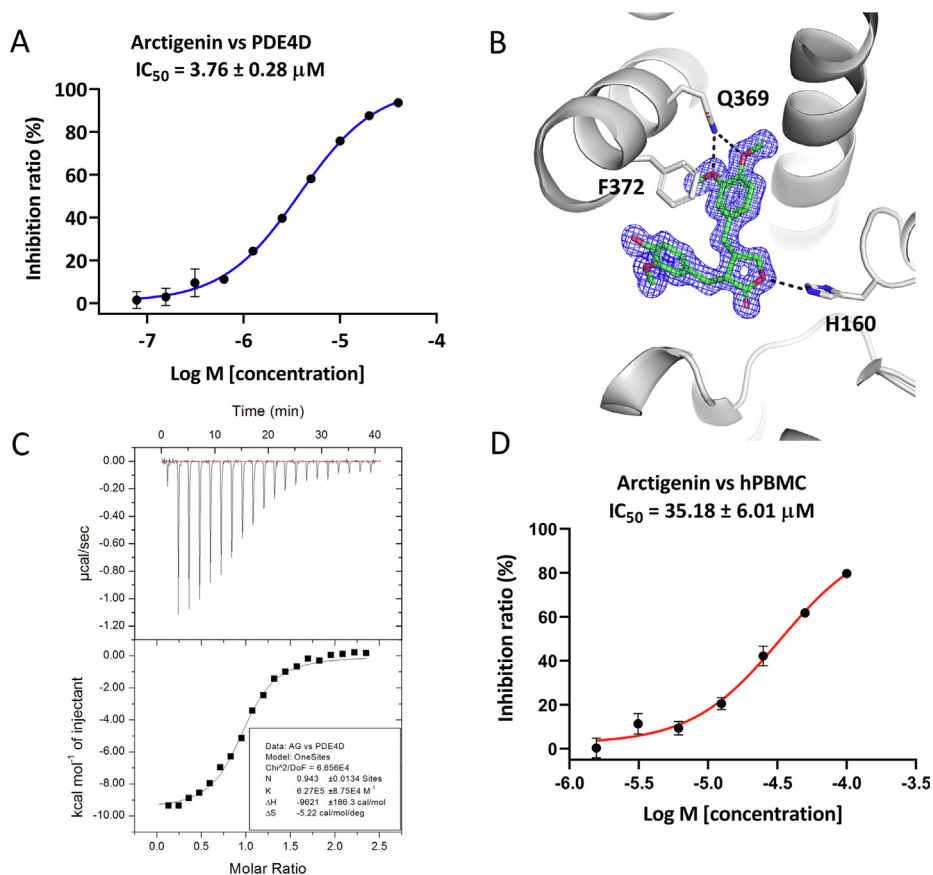
Fig. 1. Inhibitory activity of arctigenin against PDE4D and ligand binding identification revealed by ITC and X-ray crystallography. (A) Inhibitory activity of arctigenin against PDE4D catalytic domain. (B) Detailed interactions of arctigenin (green stick) with PDE4D (grey cartoon). Black dash lines indicate hydrogen bonds between ligand and residues. $2Fo\text{-}Fc$ electron density map contoured at 1σ is presented as blue mesh. (C) ITC profiles for the binding of arctigenin to PDE4D catalytic domain. (D) Inhibitory activity of arctigenin on LPS-induced production of TNF-α in human PBMCs. Data were shown as means ± SEM (n = 3).

inflammatory cytokines and promote the secretion of IL-10 (Fig. 3I). These data collectively suggested that topical application of arctigenin showed excellent therapeutic capacity for psoriatic inflammation.

Arctigenin rectified the immune dysfunction and hyperactivation of keratinocytes in the skin microenvironment

To fully reveal the pathological changes at molecular levels, the skin samples were collected and analyzed for TMT[10]-labeling quantitative proteomic analysis (Fig. 4A). Principle component analysis (PCA) displayed that vehicle group were clearly separated from normal group and arctigenin-treated group by the first principle components which declared 34.82% of the variability of the identified proteins (Fig. 4B). In our analysis, there were 806 differentially expressed proteins between normal and vehicle group; 134 proteins between vehicle and arctigenin-treated groups (Fig. 4C). Among these proteins, by contrast to vehicle group, 41 proteins were upregulated in the arctigenin group, whereas 93 proteins were downregulated (Fig. 4D), which were also demonstrated in the volcano plot (Fig. 4E). Hierarchical cluster analysis of differential protein expression level demonstrated that compared with vehicle group, arcitgenin-treated group displayed a specific cluster, which predicting the profound proteomic changes between vehicle and arcitgenin-treated group (Fig. 4F).

As illustrated in Fig. 4G, Correlation analysis of differentially expressed proteins, using Pearson algorithm, indicated that there existed an extreme close association between multiple proteins. Further functional analyses of differentially expressed proteins

were performed to excavate gene ontology (GO) annotation, including the cellular component, biological process, and molecular function (Fig. S4A). From the top30 GO term, the differential proteins were mainly linked to toll-like receptor signaling, secretion and activity of inflammatory cytokines, regulation of MAPK cascade, expression of keratin filaments (Fig. S4A). Comparison of differential proteins and all proteins in GO level 2 further confirmed that cell adhesion and junction, immune system process, extracellular matrix, antioxidant, and chemoattractant activity largely and differentially appeared in vehicle and arctigenin-treated group (Fig. S4B and Table S8). Moreover, KEGG pathway enrichment of differential proteins also referred to the immune dysfunction and hyperproliferation and abnormal activation of cells in the skin microenvironment (Fig. S4C). The network between vehicle and arctigenin-treated group was visualized by Cytoscape 3.1.1 (Fig. S4D). According to the Score Sequest HT of differentially expressed proteins, Keratin 14 attracted our attention with the highest score (1413.7). Enlightened by the findings, we naturally focused on the proteins possessing the interaction with Keratin 14 in the PPI network (Fig. S4E), which were further confirmed by the mRNA expression level of these proteins, including keratin 6, keratin 8, MMP3, Adgre1, and Integrin M (Fig. S4F).

Arctigenin modulated the PDE4-mediated signaling and attenuated the inflammatory responses in the local skin lesions

Given the critical role of PDE4 in regulating multiple inflammatory processes, we then uncovered the pathological role of PDE4 in IMQ-induced psoriasis. The results demonstrated that increased
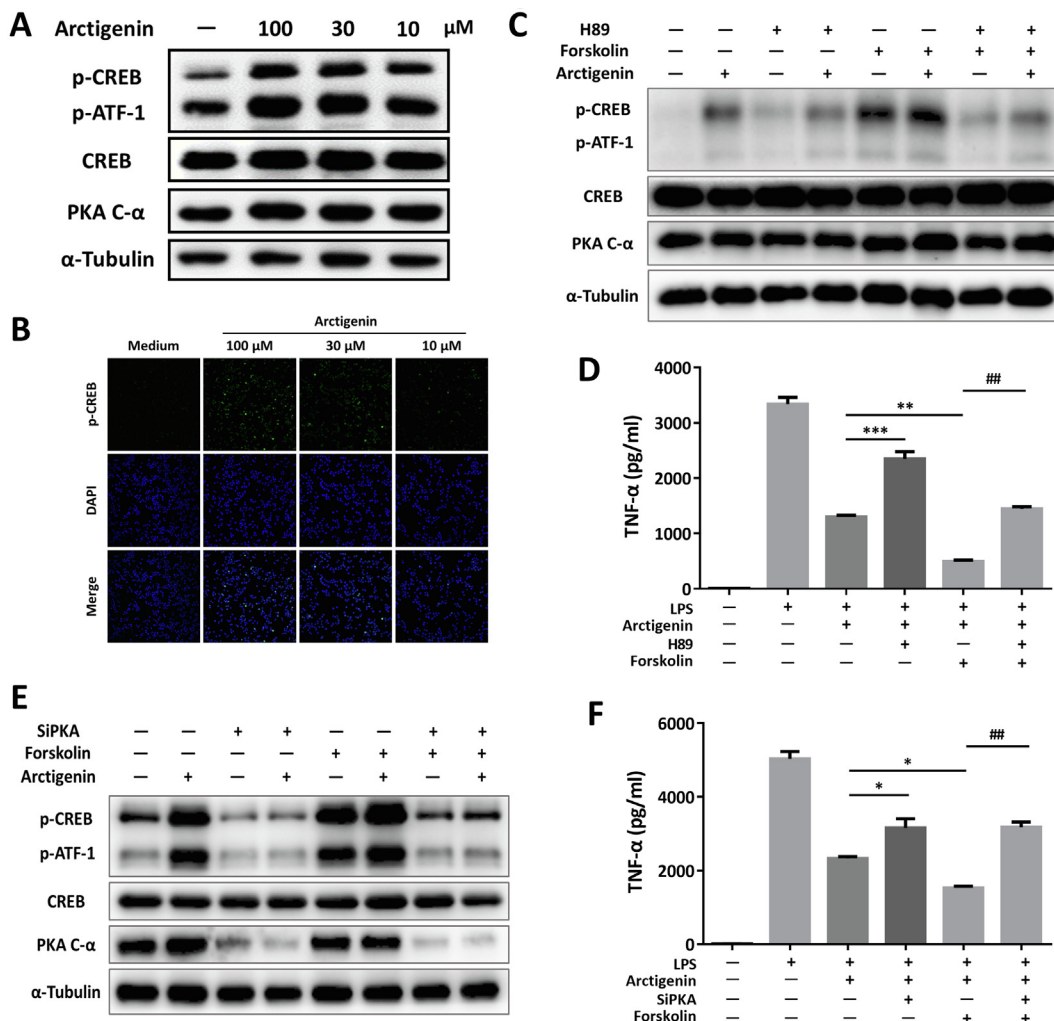
Fig. 2. PKA exerted as an indispensable factor for anti-inflammation of arctigenin in RAW264.7 cells. (A) Cells were treated with arctigenin for 15 min and collected for detection of phosphor-CREB by western blot. (B) Immunofluorescence of phospho-CREB in RAW264.7 cells. (C) Arctigenin, H89, and forskolin incubated RAW264.7 cells were analyzed for phosphor-CREB by western blot. (D) TNF-α level in RAW264.7 cells. (E) siPKA-transfected RAW264.7 cells were incuabted with arctigenin and/or forskolin, and then analyzed by western blotting. (F) TNF-α level in transfected RAW264.7 cells. All data were shown as means ± SEM (n = 3). $^*p < 0.05$, $^{**}p < 0.01$, and $^{***}p < 0.001$.

activity of cAMP-specific PDEs was observed in the vehicle mice, which could be obviously reversed by arctigenin treatment (Fig. 5A). Consistently, arctigenin could upregulate the skin level of cAMP (Fig. 5B) and promote the phosphorylation of CREB (Fig. 5E). In accordance with the results from RAW264.7 cells, arctigenin could inhibit the enzymatic activity of PDE4 in the concentration-dependent manner (Fig. 5C-D). As a consequence, arctigenin extensively attenuated the expression of several inflammatory cytokines (Fig. 5F).

To confirm the results of proteomics and fully uncover the local inflammatory microenvironments in the inflamed biopsies, the skin single-cell suspensions were determined by flow cytometric analysis. Skin-infiltrated leukocytes (CD45$^+$), antigen-presenting cells (APCs, CD45$^+$MHC II$^+$), T cells (CD45$^+$CD3$^+$), and $\gamma\delta$T cells (CD3$^+\gamma\delta$TCR$^+$) were reduced upon arctigenin treatment (Fig. S5A-B), which were also found in the skin sections staining with CD3 (Fig. S5C). Further analysis of innate immune cells demonstrated that monocytic myeloid cells (CD11b$^+$), macrophages (CD11b$^+$-F4/80$^+$), neutrophils (CD11b$^+$Gr-1$^+$), and DCs (CD11b$^+$CD11c$^+$) were largely accumulated in the vehicle group, which were decreased when treated with arctigenin (Fig. S5D). In line with inflammatory recruitment, arctigenin suppressed the protein expression of CCR6 and CXCR3 on CD45$^+$ leukocytes analyzed by flow cytometry

(Fig. S5E). Additionally, gene expression levels of multiple inflammatory mediators and chemokines, including RANTES, iNOS, MIP-1α, MIP-1β, MIG, and MIP-3α, were obviously elevated during induction of psoriasis and treatment with arctigenin could suppress the expression of chemokines in inflamed skins (Fig. S5F-G).

Discussion

The bioactive lignans, arctigenin and its mono-glycoside, arctiin, are mainly derived from the medicinal herb *Arctium lappa* L. and have been frequently investigated in multiple inflammatory diseases [4]. Previously, arctigenin was effective in relieving the experimental symptoms of pulmonary inflammation and tissue damage, mainly related to inhibition of PI3K/AKT, MAPK, and iNOS signaling pathway [5,7,33]. Recently, A phase I single dose study was designed to determine the maximum tolerated dose (or recommended dose) and bioavailability of arctigenin in healthy volunteers (*Clinicaltrials.gov.*, NCT03703388). Though arctigenin demonstrated broad modulatory effects in various disease models, the potential target remains unclear and ill-defined. In our research, PDE4-targeted ligand screening based on our in-house natural products library led to the discovery of arctigenin as novel inhibitors of PDE4 with a single digit micromolar potency. A fur-
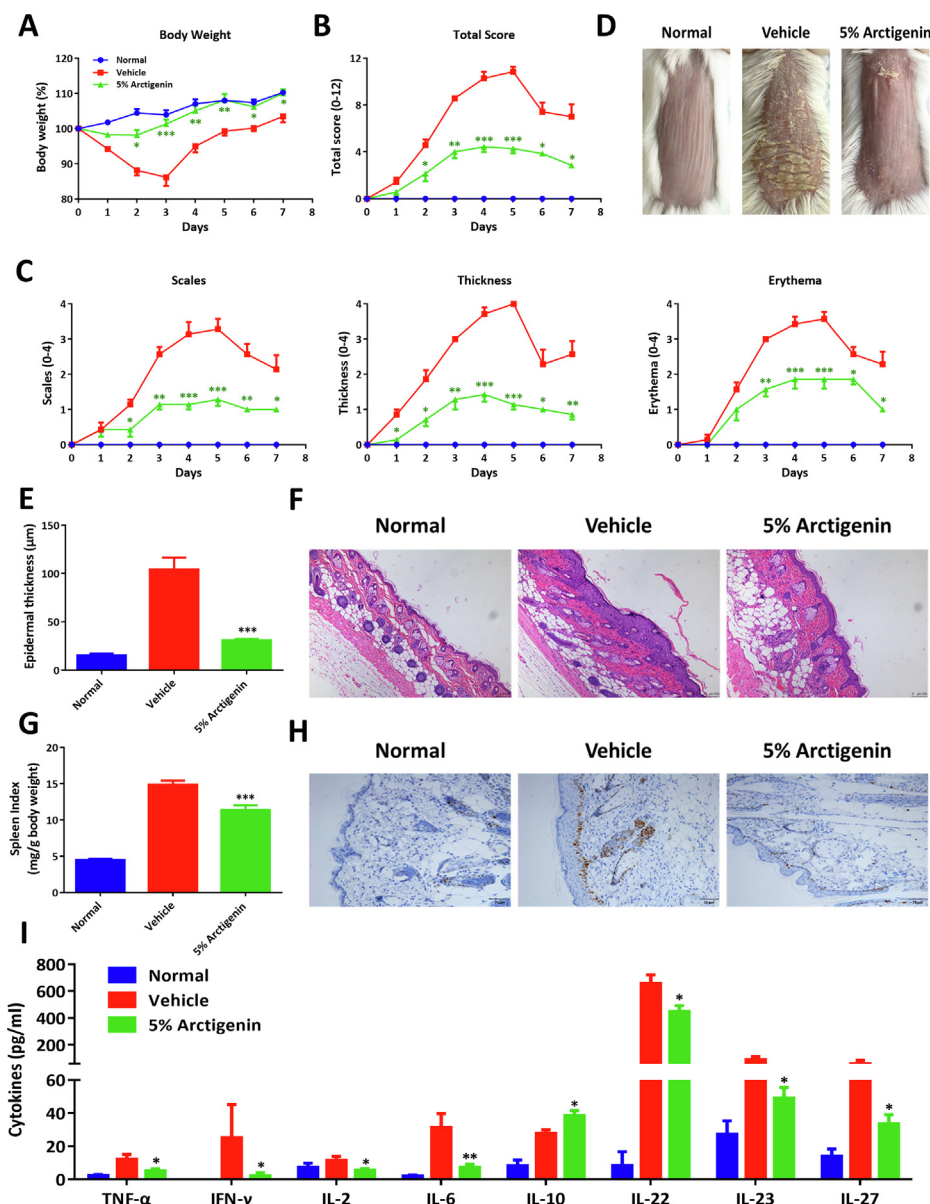
Fig. 3. Topical application of arctigenin ameliorated experimental murine psoriatic skin lesions. (A) BALB/c mice were acquired with IMQ cream and treated daily with 5% arctigenin cream and body weight changes (exhibited as the percentage of the initial weight) were monitored daily. (B) Skin PASI total scores. (C) Skin inflammatory scores, including scales, thickness, and erythema. (D) The representative manifestations of the back skins. (E) Epidermal thicknesses, acquired from H&E staining. (F) The typical H&E staining pictures of tissue slices (100 × magnification). (G) Spleen index, referring to spleen weight (mg)/body weight (g). (H) The representative immunohistochemistry staining of Ki-67 in skin slices (200 × magnification). (I) Serum cytokines, quantified by Luminex assay. All data were shown as means ± SEM; n = 7 mice per group. $*p < 0.05$, $**p < 0.01$, and $***p < 0.001$, compared with IMQ-treated mice.

ther crystallography together with thermodynamic study illuminated that arctigenin could bind to the catalytic domain of PDE4D with a typical binding conformation and with a single digit micromolar binding affinity (Fig. 1 and Table S4-S6). To our knowledge, this is the first study which clearly demonstrates the detailed molecular mechanisms of arctigenin binding to a specific target protein in modulating inflammation (Fig. 6).

Over the past few decades, numerous PDE4 inhibitors have been designed in the field of autoimmune and inflammation-related diseases [19]. However, due to the unexpected permeability of blood–brain barrier and other severe adverse effects, a large number of PDE4 inhibitors were impeded and restricted in further applications [17,26]. It is worth informing that the tissue accumulation of arctigenin in brain was lower than that in intestine, liver, kidney, lung, and heart, which might account for the safety profile of

arctigenin [34]. In addition, following oral administration, the $t_{1/2}$ was short (<2h) and the plasma concentration of arctigenin was even undetectable in several animal species, which substantially hindered the therapeutic efficacies *in vivo* [4,35]. Therefore, there is an urgent need for alternative dosing procedures to improve systemic or target organ exposure. Unlike systemic treatment, topical application might directly touch the inflamed positions and result in higher drug concentration in skin than that by oral administration. Accordingly, we indeed found that topical treatment of 5% arctigenin cream showed a better therapeutic effect than oral administration of 100 mg/kg arctigenin (Fig. S6). Significantly, arctigenin has a good transdermal absorption, and a high concentration of arctigenin could be detected in the inflamed skin tissues (29.67 ± 15.42 μg/g skin samples), which further ensures the therapeutic effect of arctigenin in treating psoriasis.
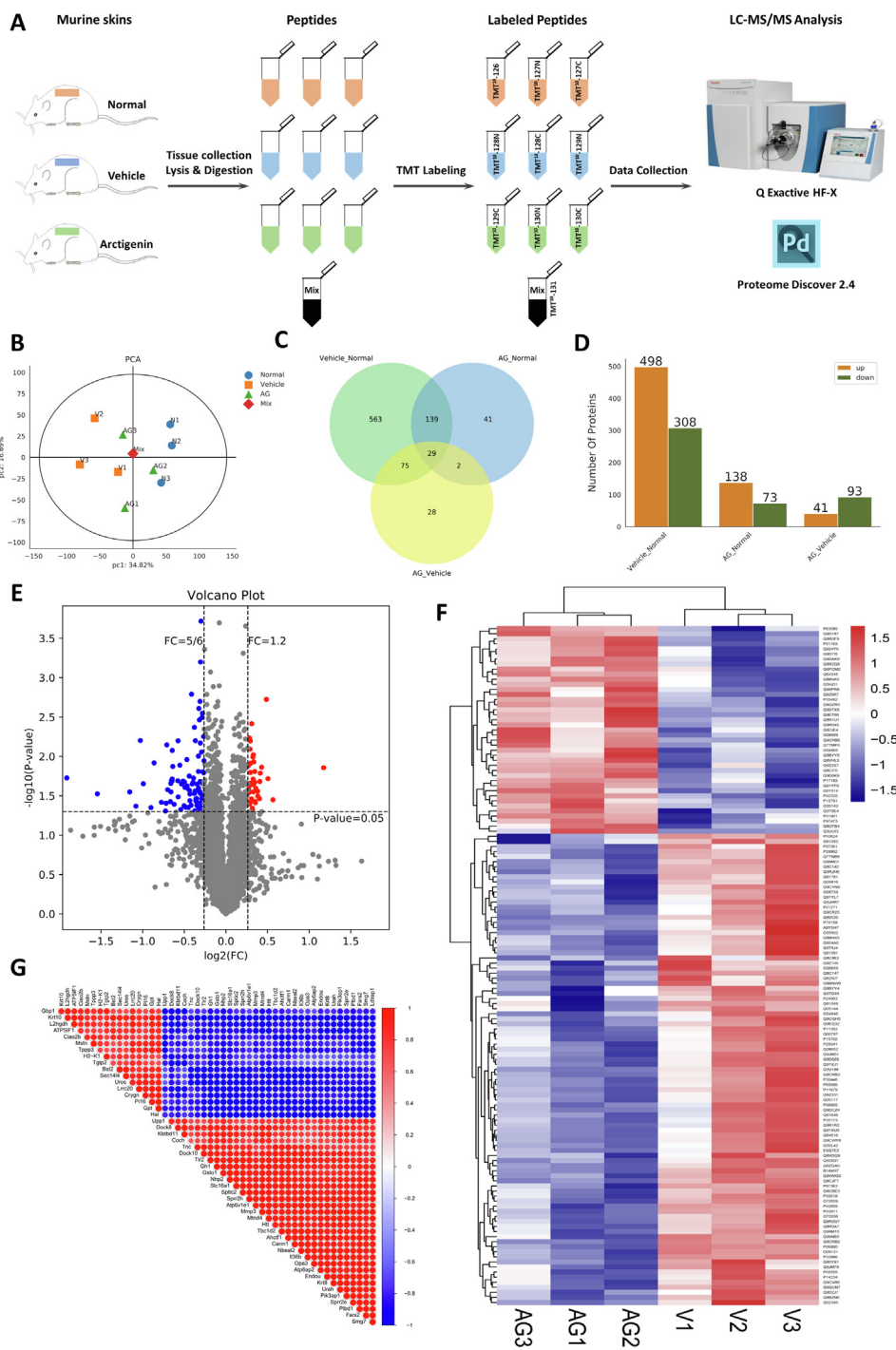
Fig. 4. Quantitative proteomic analysis of arctigenin-intervened psoriatic skin lesions. (A) Flow chart of the TMT-labeled quantitative proteomic study on murine skin samples. (B) The principle component analysis (PCA) of three groups. (C) Venn diagram indicated the shared and uniquely identified proteins in three groups. (D) Number of differential expressed proteins of different groups and the protein which meet the requirements (Foldchange = 1.2 and p-value < 0.05) is listed. (E) Volcano plot of differential expressed proteins between vehicle and arctigenin-treated vehicle mice. (F) Cluster analysis of differential protein expression level in vehicle and arctigenin-treated vehicle mice. (G) Correlation analysis of protein expression (Top50 significantly different proteins between vehicle mice (IMQ-treated only) and arctigenin-treated vehicle mice).

Psoriasis is an inflammatory skin disease involving immune cells and innate and adaptive immune molecules [36,37]. The pathogenesis of psoriasis is multifactorial and complicated, and is often associated with genetic susceptibility, disorders of the skin's microbes and immune system, and environmental triggers [20]. To fully understand the histopathological changes at the protein levels, TMT[10]-labeling quantitative proteomic analysis was performed to uncover the potential mechanism. There existed unique distribution patterns among three groups from PCA analysis and

differentially expressed proteins were identified between vehicle and arctigenin-treated groups (Fig. 4B-F). Further functional analyses of differentially expressed proteins, including GO annotation and KEGG PPI network, suggested that the potential mechanism of arctigenin, from the protein level, were mainly related to toll-like receptor signaling, activity of inflammatory cytokines, antioxidant and chemoattractant activity, and expression of keratin filaments (Fig. S4A-B). Keratinocytes, the prominent parenchyma cell in the skin epidermis, function as the impressive barrier to
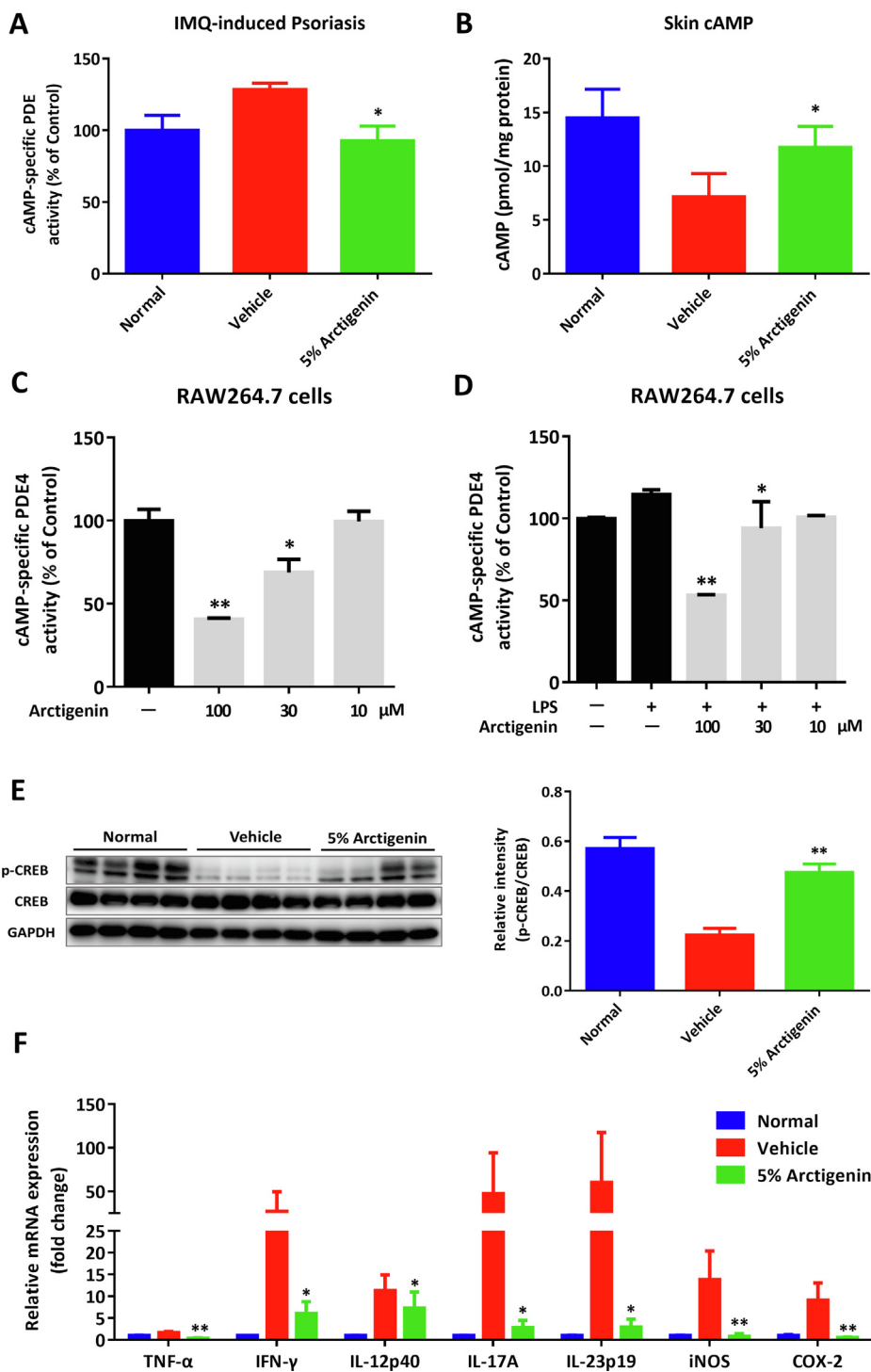
Fig. 5. Arctigenin suppressed the PDE4-mediated inflammation in IMQ-induced psoriasis. (A) The enzymatic activity of cAMP-specific PDE in skins. (B) The cAMP levels in skins. (C) The enzymatic activity of cAMP-specific PDE4 in RAW264.7 cells and LPS-stimulated RAW264.7 cells (D). (E) Western blotting assay of phosphorylation of CREB in skins. (F) The mRNA level of cytokines in the inflamed tissues. All data were shown as means ± SEM; n = 7 mice per group. *$p < 0.05$, **$p < 0.01$, and ***$p < 0.001$, compared with IMQ-treated mice.

separate internal components from external stimuli; Meanwhile, keratins form the predominant intermediate filament cytoskeleton of keratinocytes, in which keratins represent the major constituent of proteins in keratinocytes [38]. Previous reports have indicated hyperproliferation-associated keratins were considered to be the hallmarks of psoriasis [39,40]. Among those proteins, Keratin 14 and its associated proteins, including keratin6, keratin8, MMP3, Adgre1, and Integrin M, mostly functioned in the

progression of psoriasis and the process of arctigenin treatment (Fig. S4C-F).

Conclusion

The present research indicated that arctigenin could occupy the catalytic binding site of PDE4D and showed inhibitory activity
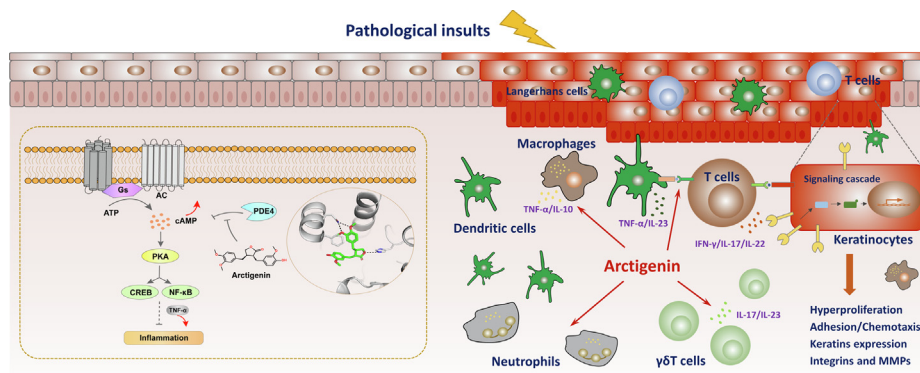
Fig. 6. Schematic illustration of the effects of arctigenin, as a potent PDE4 inhibitor, involved in attenuating psoriatic skin inflammation.

against the degradation of cAMP for the first time. As a result, arctigenin displayed dramatic anti-inflammation in LPS-primed human PBMCs and murine RAW264.7 cells, which was largely owing to activation of the cAMP-dependent PKA-CREB signaling. Further proteomics research confirmed that arctigenin could rectify the immune dysfunction and hyperactivation of keratinocytes in the inflamed skin microenvironments, which might be largely associated with the expression of Keratin 14. In sum, our study provided the credible evidence that inhibition of PDE4 by arctigenin might function as the potential therapeutic approach in treating inflammatory disorders.

Author contributions

H Li, XL Zhang, W Tang, and YC Xu designed the study. H Li, XL Zhang, CG Xiang, MT Liu, HM Lu, CL Feng, C Fan, HX Su, Y Zhou, and Q Qi performed the experiments. H Li and XL Zhang analyzed the experimental data and contributed to writing the manuscript. W Tang and YC Xu obtain the funding and revised the manuscript. All authors approved the final version of the manuscript.

Compliance with ethics requirements

Female BALB/c mice (6–8 weeks, 20–22 g) were acquired from Shanghai Laboratory Animal Center of the Chinese Academy of Sciences. All experiments were carried out according to the National Institutes of Health Guide for Care and Use of Laboratory Animals in compliance with the ARRIVE guidelines and were approved by the Bioethics Committee of the Shanghai Institute of Materia Medica (IACUC: 2018–03-ZJP-70).

Declaration of Competing Interest

The authors declared that there is no conflict of interest.

Acknowledgements

Appendix A. Supplementary data

Supplementary data to this article can be found online at https://doi.org/10.1016/j.jare.2021.02.006.

References

[1] Tsai YF, Yu HP, Chung PJ, Leu YL, Kuo LM, Chen CY, et al. Osthol attenuates neutrophilic oxidative stress and hemorrhagic shock-induced lung injury via inhibition of phosphodiesterase 4. Free Radical Biol. Med. 2015;89:387–400.

[2] Tsai YF, Chu TC, Chang WY, Wu YC, Chang FR, Yang SC, et al. 6-Hydroxy-5,7-dimethoxy-flavone suppresses the neutrophil respiratory burst via selective PDE4 inhibition to ameliorate acute lung injury. Free Radical Biol. Med. 2017;106:379–92.

[3] Sengupta S, Mehta G. Natural products as modulators of the cyclic-AMP pathway: evaluation and synthesis of lead compounds. Org. Biomol. Chem. 2018;16(35):6372–90.

[4] Gao Q, Yang M, Zuo Z. Overview of the anti-inflammatory effects, pharmacokinetic properties and clinical efficacies of arctigenin and arctiin from Arctium lappa L. Acta Pharmacol. Sin. 2018;39(5):787–801.

[5] Zhou B, Weng G, Huang Z, Liu T, Dai F. Arctiin Prevents LPS-Induced Acute Lung Injury via Inhibition of PI3K/AKT Signaling Pathway in Mice. Inflammation 2018;41(6):2129–35.

[6] Cheng X, Wang H, Yang J, Cheng Y, Wang D, Yang F, et al. Arctigenin protects against liver injury from acute hepatitis by suppressing immune cells in mice. Biomed. Pharmacother. 2018;102:464–71.

[7] Shi X, Sun H, Zhou D, Xi H, Shan L. Arctigenin attenuates lipopolysaccharide-induced acute lung injury in rats. Inflammation 2015;38(2):623–31.

[8] Feng Q, Yao J, Zhou G, Xia W, Lyu J, Li X, et al. Quantitative Proteomic Analysis Reveals That Arctigenin Alleviates Concanavalin A-Induced Hepatitis Through Suppressing Immune System and Regulating Autophagy. Front. Immunol. 2018;9:1881.

[9] Wu X, Dou Y, Yang Y, Bian D, Luo J, Tong B, et al. Arctigenin exerts anti-colitis efficacy through inhibiting the differentiation of Th1 and Th17 cells via an mTORC1-dependent pathway. Biochem. Pharmacol. 2015;96(4):323–36.

[10] Wu X, Yang Y, Dou Y, Ye J, Bian D, Wei Z, et al. Arctigenin but not arctiin acts as the major effective constituent of Arctium lappa L. fruit for attenuating colonic inflammatory response induced by dextran sulfate sodium in mice. Int. Immunopharmacol. 2014;23(2):505–15.

[11] Hyam SR, Lee IA, Gu W, Kim KA, Jeong JJ, Jang SE, et al. Arctigenin ameliorates inflammation in vitro and in vivo by inhibiting the PI3K/AKT pathway and polarizing M1 macrophages to M2-like macrophages. Eur. J. Pharmacol. 2013;708(1–3):21–9.

[12] Li W, Zhang Z, Zhang K, Xue Z, Li Y, Zhang Z, et al. Arctigenin Suppress Th17 Cells and Ameliorates Experimental Autoimmune Encephalomyelitis Through AMPK and PPAR-gamma/ROR-gammat Signaling. Mol. Neurobiol. 2016;53 (8):5356–66.

[13] Motte E, Le Stunff C, Briet C, Dumaz N, Silve C. Modulation of signaling through GPCR-cAMP-PKA pathways by PDE4 depends on stimulus intensity: Possible implications for the pathogenesis of acrodysostosis without hormone resistance. Mol. Cell. Endocrinol. 2017;442:1–11.

[14] Oger S, Mehats C, Dallot E, Cabrol D, Leroy MJ. Evidence for a role of phosphodiesterase 4 in lipopolysaccharide-stimulated prostaglandin E2 production and matrix metalloproteinase-9 activity in human amniochorionic membranes. J. Immunol. 2005;174(12):8082–9.

[15] Schafer PH, Truzzi F, Parton A, Wu L, Kosek J, Zhang LH, et al. Phosphodiesterase 4 in inflammatory diseases: Effects of apremilast in psoriatic blood and in dermal myofibroblasts through the PDE4/CD271 complex. Cell. Signal. 2016;28(7):753–63.

[16] Li H, Fan C, Feng C, Wu Y, Lu H, He P, et al. Inhibition of phosphodiesterase-4 attenuates murine ulcerative colitis through interference with mucosal immunity. Br. J. Pharmacol. 2019;176(13):2209–26.

[17] Maurice DH, Ke H, Ahmad F, Wang Y, Chung J, Manganiello VC. Advances in targeting cyclic nucleotide phosphodiesterases. Nat. Rev. Drug Discov. 2014;13 (4):290–314.

[18] Spina D. PDE4 inhibitors: current status. Br. J. Pharmacol. 2008;155(3):308–15.

[19] Li H, Zuo J, Tang W. Phosphodiesterase-4 Inhibitors for the Treatment of Inflammatory Diseases. Front. Pharmacol. 2018;9:1048.

[20] Pasparakis M, Haase I, Nestle FO. Mechanisms regulating skin immunity and inflammation. Nat. Rev. Immunol. 2014;14(5):289–301.

[21] Luster AD, Alon R, von Andrian UH. Immune cell migration in inflammation: present and future therapeutic targets. Nat. Immunol. 2005;6(12):1182–90.

[22] Bowcock AM, Krueger JG. Getting under the skin: the immunogenetics of psoriasis. Nat. Rev. Immunol. 2005;5(9):699–711.

[23] Veldhoen M. Interleukin 17 is a chief orchestrator of immunity. Nat. Immunol. 2017;18(6):612–21.

[24] Gaffen SL, Jain R, Garg AV, Cua DJ. The IL-23-IL-17 immune axis: from mechanisms to therapeutic testing. Nat. Rev. Immunol. 2014;14 (9):585–600.

[25] Zhang X, Dong G, Li H, Chen W, Li J, Feng C, et al. Structure-Aided Identification and Optimization of Tetrahydro-isoquinolines as Novel PDE4 Inhibitors Leading to Discovery of an Effective Antipsoriasis Agent. J. Med. Chem. 2019;62(11):5579–93.

[26] Li H, Li J, Zhang X, Feng C, Fan C, Yang X, et al. DC591017, a phosphodiesterase-4 (PDE4) inhibitor with robust anti-inflammation through regulating PKA-CREB signaling. Biochem. Pharmacol. 2020;177. 113958.

[27] van der Fits L, Mourits S, Voerman JS, Kant M, Boon L, Laman JD, et al. Imiquimod-induced psoriasis-like skin inflammation in mice is mediated via the IL-23/IL-17 axis. J. Immunol. 2009;182(9):5836–45.

[28] Byamba D, Kim DY, Kim DS, Kim TG, Jee H, Kim SH, et al. Skin-penetrating methotrexate alleviates imiquimod-induced psoriasiform dermatitis via decreasing IL-17-producing gamma delta T cells. Exp. Dermatol. 2014;23 (7):492–6.

[29] Shibata S, Tada Y, Hau CS, Mitsui A, Kamata M, Asano Y, et al. Adiponectin regulates psoriasiform skin inflammation by suppressing IL-17 production from gammadelta-T cells. Nat. Commun. 2015;6:7687.

[30] Fang R, Cui Q, Sun J, Duan X, Ma X, Wang W, et al. PDK1/Akt/PDE4D axis identified as a target for asthma remedy synergistic with beta2 AR agonists by a natural agent arctigenin. Allergy 2015;70(12):1622–32.

[31] Zhao F, Wang L, Liu K. In vitro anti-inflammatory effects of arctigenin, a lignan from Arctium lappa L., through inhibition on iNOS pathway. J. Ethnopharmacol. 2009;122(3):457–62.

[32] Xin W, Tran TM, Richter W, Clark RB, Rich TC. Roles of GRK and PDE4 activities in the regulation of beta2 adrenergic signaling. J. Gen. Physiol. 2008;131 (4):349–64.

[33] Zhang WZ, Jiang ZK, He BX, Liu XB. Arctigenin Protects against Lipopolysaccharide-Induced Pulmonary Oxidative Stress and Inflammation in a Mouse Model via Suppression of MAPK, HO-1, and iNOS Signaling. Inflammation 2015;38(4):1406–14.

[34] Li J, Li X, Ren YS, Lv YY, Zhang JS, Xu XL, et al. Elucidation of Arctigenin Pharmacokinetics and Tissue Distribution after Intravenous, Oral, Hypodermic and Sublingual Administration in Rats and Beagle Dogs: Integration of In Vitro and In Vivo Findings. Front. Pharmacol. 2017;8:376.

[35] Ikeda M, Sato A, Mochizuki N, Toyosaki K, Miyoshi C, Fujioka R, et al. Phase I trial of GBS-01 for advanced pancreatic cancer refractory to gemcitabine. Cancer Sci. 2016;107(12):1818–24.

[36] Li H, Lu H, Tang W, Zuo J. Targeting methionine cycle as a potential therapeutic strategy for immune disorders. Expert Opin. Ther. Targets 2017;21(9):861–77.

[37] Benhadou F, Mintoff D, del Marmol V. Psoriasis: Keratinocytes or Immune Cells – Which Is the Trigger?. Dermatology 2019;235(2):91–100.

[38] Tamilselvi E, Jingying S, Caihong Z, Fusheng Z, Yaohua Z, Liangdan S, et al. Mutational analysis of epidermal and hyperproliferative type I keratins in mild and moderate psoriasis vulgaris patients: a possible role in the pathogenesis of psoriasis along with disease severity. Hum. Genomics 2018;12(1):27.

[39] Ippagunta SK, Gangwar R, Finkelstein D, Vogel P, Pelletier S, Gingras S, et al. Keratinocytes contribute intrinsically to psoriasis upon loss of *Tnip1* function. Proc. Natl. Acad. Sci. U. S. A. 2016;11341:E6162–71.

[40] Yang L, Fan X, Cui T, Dang E, Wang G. Nrf2 promotes keratinocyte proliferation in psoriasis through up-regulation of Keratin 6, Keratin 16 and Keratin 17. J. Invest. Dermatol. 2017;137(10):2168–76.